NUMERICAL STUDY ON ELECTROPHORETIC MOTION OF A BIO-POLYMER THROUGH A NANO-PORE

Suresh Alapati[1] and Yong Kweon Suh[*2]

나노 세공을 통한 비드 체인의 전기영동에 관한 수치해석적 연구

수레수 알라파티,[1] 서 용 권[*2]

In this work, the electrophoretic motion of dsDNA molecule represented by a polymer through an artificial nano-pore in a membrane is simulated using the numerical method combining the lattice Boltzmann and Langevin molecular dynamic method. The polymer motion is represented by Langevin molecular dynamics technique while the fluid flow is taken into account by fluctuating lattice-Boltzmann method. The hydrodynamic interactions between the polymer and solvent in a confined space with a membrane having a hole are considered explicitly through the frictional and the random forces. The electric field intensity over the space is obtained from a finite difference method. Initially, the polymer is placed at one side of the space, and an electric field is applied to drive the polymer to the other side of the space through the nano-pore. In future, we plan to study the effect of the polymer size and the electric field on the electrophoretic velocity.

Key Words : Multi-Dynamics, Bio-Polymer, Nano-Pore, Numerical Simulation, Langevin Dynamics

1. INTRODUCTION

Translocation of bio-polymer molecules through nanometer sized pores in a membrane is one of the most fundamental processes in the fields of chemistry and biotechnology. This event often takes place in several biological processes such as DNA and RNA sequencing, proteins transporting trough a cell membrane, transfer of virus RNA to the host cells, gene therapy, electrophoresis, and delivery of drug molecules to their activation sites, etc. Therefore understanding the translocation phenomenon might lead to developing new and improved techniques for biological applications. Many researchers paid considerable attention to understanding the underlying physics, theoretically, experimentally and numerically. Theoretical predictions of translocation dynamics are very difficult as there are so many factors affecting the entire process. The main factors that affect the translocation process are: interaction among monomers in the polymer chain, hydrodynamic interactions, driving forces associated with electrical or chemical potential difference, concentration gradient of the polymer, the pore size and the polymer length. Hydrodynamic interaction (interaction with solvent molecules) plays an important role in the dynamics of the biopolymer translocation process. If we completely rely on molecular dynamics techniques to take the hydrodynamic interaction into account, we have to consider so many solvent molecules even for a small number of polymer particles and the time scale of simulation should be set so small (in pico seconds). Most of the computational time is spent on details of the solvent which are not of our concern as far as the polymer motion is concerned. To deal with this type of problem, multiscale-modeling techniques are developed which are known to reduce the computational time up to two orders of magnitude [1-5]. In these techniques the solvent is modeled on the continuum basis and the polymer is modeled by standard

1 정회원, 동아대학교 대학원 기계공학과
2 정회원, 동아대학교 기계공학과
* Corresponding author, E-mail: yksuh@dau.ac.kr

molecular dynamic (MD) techniques. The polymer and the solvent are coupled through a simple dissipative (hydrodynamic) force. There are so many mesoscopic methods available for simulating solvent dynamics on the continuum basis. Some of them are Brownian dynamics [1], dissipative particle dynamics [2], multi-particle collision dynamics [3], and lattice Boltzmann equation (LBE) [4,-5]. Each of these methods has its own strengths and weaknesses. The advantage of LBE over other methods is that computational cost of taking the hydrodynamic interactions scales only linearly with the polymer length. Further the complex boundaries can be easily handled with LBE.

Our main objectives in this study are to evaluate numerically, by using LBE, how the hydrodynamic interaction influences the electrophoretic motion of a polymer representing a DNA through a nano-pore and to determine the scaling of the translocation time with the chain length. The paper is organized as follows: The details of numerical method are given in Section 2. The results obtained from the simulation of translocation process are presented in Section 3. Finally, in Section 4 the conclusions of the present study and the scope of future work are drawn.

2. NUMERICAL METHOD

2.1 DNA MOTION - BEAD-SPRING MODEL

The DNA is represented on coarse-grained level by a bead-spring model, which consists of N monomer units (also known as beads, each bead corresponding to several base pairs) connected by N-1 springs. The force acting on a bead i can be represented by the generalized Langevin equations of motion in terms of the bead positions $\boldsymbol{r_i}$ and velocity $\boldsymbol{v_i}$ for i=1,…,N,

$$\frac{d\boldsymbol{r_i}}{dt}=\boldsymbol{v_i} \tag{1a}$$

$$m_i\frac{d\boldsymbol{v_i}}{dt}=-\frac{\partial\vartheta_{tot}}{\partial\boldsymbol{r_i}}+\boldsymbol{F_{drag,i}}+\boldsymbol{F_{ran,i}} \tag{1b}$$

where m_i is the mass of the bead, t is the time, ϑ_{tot} denotes the total potential energy of the system, which is the sum of the total Lennard-Jones potential, i.e. sum of $V_{LJ}(r_{ij})$ over all the other beads, the bond stretching potential $V_{bond}(r_{ij})$ between two neighboring beads, the bond angle potential $V_{bend}(\theta)$ caused by the bending of two neighboring links, and the external electric potential $V_{el}(\boldsymbol{r_i})$ times the charge of the bead. Here r_{ij} is a scalar, i.e., the distance between a pair of interacting particles i and j, and θ is the angle between two links consecutively connecting three neighboring beads. $\boldsymbol{F_{drag,i}}$ in Eq. (1b) represents the viscous drag force due to the relative motion of the polymer in a solvent (fluid), which is given by

$$\boldsymbol{F_{drag,i}}=-\Gamma(\boldsymbol{v_i}-\boldsymbol{u_i}) \tag{2}$$

where Γ the friction coefficient and $\boldsymbol{u_i}$ the velocity of the fluid evaluated at the bead position. If there is no hydrodynamic interactions effect, we just set $\boldsymbol{u_i}=0$. The last term in Eq. (1b) is a random force due to the thermal fluctuations in the fluid environment, which is taken as a Gaussian random variable with the mean and the variance is given by

$$\begin{aligned}&<\boldsymbol{F_{ran,i}}>=0,\\&<\boldsymbol{F_{ran,i}}\boldsymbol{F_{ran,j}}>=2k_BT\Gamma\delta_{ij}\delta(t-t').\end{aligned} \tag{3}$$

The random force is uncorrelated between beads and in time as denoted by the Kronecker delta function δ_{ij} and the Dirac-delta function $\delta(t-t')$ in Eq. (3). The random force term defined in this way acts as a thermostat which keeps the temperature of the polymer at a particular value T, which is the same as that of the fluid. Note that the variance in Eq. (3) must be coupled to the friction coefficient in order to satisfy the fluctuation dissipation theorem (FDT); see [6] for the details.

The excluded volume interaction between the bead-bead and the bead-wall is taken into account by standard 6-12 Lennard-Jones potential [7]

$$V_{LJ}(r_{ij})=\begin{cases}4\epsilon\left[\left(\frac{\sigma}{r_{ij}}\right)^{12}-\left(\frac{\sigma}{r_{ij}}\right)^{6}\right] & \text{if } r_{ij}<r_{cut}\\ 0 & \text{if } r_{ij}>r_{cut}\end{cases} \tag{4}$$

where σ, ϵ are the length and the energy scales of the interaction respectively, and $r_{cut}=2^{1/6}\sigma$ is the cut-off distance which ensures only repulsive interaction takes place when two beads are closer than r_{cut}. The connectivity between the interested bead i and the adjacent one j is treated by the bond stretching interaction potential with harmonic approximation given by

$$V_{bond}(r_{ij}) = \frac{1}{2} K_{bond}(r_{ij} - \sigma_0)^2 \quad (5)$$

where K_{bond} is the harmonic force constant and σ_0 is the predetermined equilibrium bond length between adjacent beads. To ensure a proper stiffness for the polymer chain, we include the bond angle interaction potential which can be expressed as

$$V_{bend}(\theta) = \frac{1}{2} K_{bend}(\theta - \theta_0)^2 \quad (6)$$

where K_{bend} is the bond angle force constant which restores the angle θ to an equilibrium angle θ_0; we set $\theta_0 = \pi$ in this work. The potential due to the external electric force is expressed in terms of effective charge of each bead q_i and the external electric potential $\varphi(\boldsymbol{r_i})$ as

$$V_{el}(\boldsymbol{r_i}) = q_i \varphi(\boldsymbol{r_i}). \quad (7)$$

The distribution of the electric potential inside the space $\varphi(\boldsymbol{r})$ is obtained by solving the Laplace equation $\nabla^2 \varphi = 0$ using a finite difference method with very fine grids. As boundary conditions, we apply a total potential drop, $\triangle\varphi$, across the periodic length, and $\boldsymbol{n}.\nabla\varphi = 0$ at the walls. Here $\boldsymbol{n}$ is the unit vector normal to the walls. The electric force acting on each bead is calculated from $\boldsymbol{F_{el}} = -q_i \boldsymbol{E}$, with the electric field $\boldsymbol{E}$ given by $\boldsymbol{E} = -\nabla\varphi$. The electric field at bead position is interpolated from the field values at surrounding grid points. In our simulation the electrostatic interaction between the beads is neglected as the Debye screening length of DNA is in the order of 2 nm, while the persistence length is in the order of 50 nm. Persistence length is a measure of stiffness of the polymer, the larger the persistence length indicates more stiff, and vice versa.

2.2 Fluid Motion - Lattice Boltzmann Method

In our simulation the solvent dynamics is computed by lattice Boltzmann method (LBM) [8]. In LBM, the hydrodynamic variables (density, velocity) are evaluated from the particle distribution functions, $f_n(\boldsymbol{r},t)$, by numerically solving the Boltzmann kinetic equation on a discrete lattice mesh. Here $f_n(\boldsymbol{r},t)$ represents the probability of finding a particle at lattice site $\boldsymbol{r}$ and at time t which is moving with discrete velocity $\boldsymbol{c_n}$. The particles move on a regular lattice defined by discrete

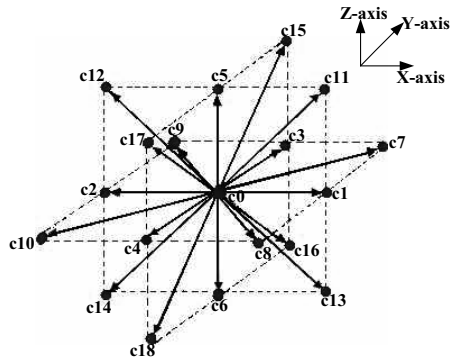

Fig. 1 D3Q19 (3D with 19 velocity vectors) lattice

velocity set $\boldsymbol{c_n}(n = 0,1,.....b)$, which is chosen such that after a time step $\triangle t$, the particle arrives at n^{th} neighboring grid point. Here we worked with a cubic lattice consisting of 19 velocity vectors in 3-dimensions (D3Q19 lattice, see Fig. 1). The evolution of f_n is governed by generalized lattice Boltzmann equation [9]:

$$f_n(\boldsymbol{r} + \boldsymbol{c_n}\triangle t, t + \triangle t) = f_n^*(\boldsymbol{r},t) = f_n(\boldsymbol{r},t) + \sum_{m=0}^{b} L_{nm}\left[f_m(\boldsymbol{r},t) - f_m^{eq}(\boldsymbol{r},t)\right] + M_n(\boldsymbol{r},t) \quad (8)$$

where L_{nm} is a collision operator due to instantaneous collisions between particles. After collision process the populations are relaxed towards local equilibrium distribution, f_n^{eq}, which can be expressed in terms of the hydrodynamic variables $\boldsymbol{u}$ and ρ (the mass density) as follows:

$$f_n^{eq}(\rho,\boldsymbol{u}) = \rho a^{c_n}\left[1 + \frac{\boldsymbol{c_n}.\boldsymbol{u}}{c_s^2} + \frac{(\boldsymbol{c_n}.\boldsymbol{u})^2}{2c_s^4} - \frac{u^2}{c_s^2}\right] \quad (9)$$

where a^{c_n} are the set of known weights which depend on the lattice model, and c_s is the speed of sound in the solvent. The last term, $M_n(\boldsymbol{r},t)$ in Eq. (8) is a result of the momentum transfer from the polymer to fluid which is explained in the following section.

2.3 Coupling of Polymer and Fluid

As the fluid exerts a drag force on each of the polymer bead (according to Eq. (2)), an equal and opposite force should be applied to the fluid to conserve the total momentum of the system. Since the fluid is

modeled on the discrete grids while the polymer moves continuously on it, the fluid velocity $\boldsymbol{u_i}$ at the bead position should be interpolated from those defined at the surrounding grid points. We employed the simple nearest grid-point interpolation technique (tri-linear interpolation) for this purpose [4]. In addition to the drag force, the random force in Eq. (3) should also be given to the fluid to satisfy FDT. Since the friction and random forces are available at the bead positions, we have to extrapolate them from the bead positions to the surrounding grid points. We used the same interpolation function that is used in the velocity interpolation. The total force density which is given to the fluid that resides on the grid point $\boldsymbol{r}$ is written as

$$\boldsymbol{f^{fl}}(\boldsymbol{r}) = -\sum_{i\in nc}(\boldsymbol{F_{drag,i}}+\boldsymbol{F_{ran,i}})w(\boldsymbol{r})/\triangle x^3 \qquad (10)$$

where $w(\boldsymbol{r})$ is the interpolation function based on the distance of the bead from the grid point and $\triangle x$ is the lattice grid spacing. Summation in Eq.(10) should be taken over all the beads included in 8 neighboring cells nc, around the grid point. The source term, $M_n(\boldsymbol{r},t)$, in Eq. (8) can be obtained from [10],

$$M_n(\boldsymbol{r},t) = \left(1-\frac{1}{2\tau}\right)\rho a^{c_n}\left[\frac{\boldsymbol{c_n}-\boldsymbol{u}}{c_s^2}+\frac{(\boldsymbol{c_n}.\boldsymbol{u})^2}{c_s^4}\boldsymbol{c_n}\right].\boldsymbol{f^{fl}}\triangle t \qquad (11)$$

where τ is the relaxation time. The fluid density and momentum are obtained from:

$$\rho = \sum_i f_i\,, \qquad \rho\boldsymbol{u} = \sum_i f_i.\boldsymbol{c_i} + \frac{\triangle t}{2}\boldsymbol{f^{fl}}. \qquad (12)$$

These are locally conserved in any collision process and the local equilibrium distribution functions should also satisfy Eq. (12).

3. Results and Discussions

3.1 Validation Tests

Before proceeding to simulation of the translocation process of the polymer, our numerical model is verified by comparing the radius of gyration of the polymer with the power law. The mean square radius of gyration is given by

$$\langle R_g^2\rangle = \frac{1}{2N^2}\sum_{ij}\langle r_{ij}^2\rangle. \qquad (13)$$

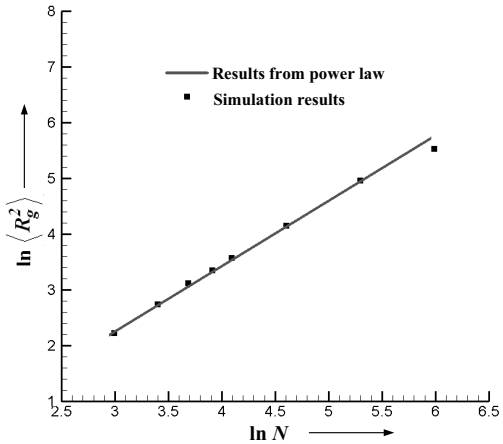

Fig.2 Numerical result of the radius of gyration of a polymer (symbols) and the data-fit line based on the power law

The radius of gyration $\langle R_g^2\rangle$ is known to be related to the number of beads N by power law as follows [11].

$$\langle R_g^2\rangle \propto N^{2\nu}, \qquad (14)$$

where ν is called the Flory exponent. For self-avoiding walk chains (with the L-J and bonding potentials activated) the Flory exponent is 0.588 [11]. We have computed $\langle R_g^2\rangle$ for several different bead numbers using Eq. (13). To attain the statistical accuracy, we calculated an ensemble average over 180 samples. Fig. 2 shows the log-log plot of $\langle R_g^2\rangle$ vs N. The symbols indicate the results obtained from the simulation, while the solid line from the data fit with a straight line based on the power law, Eq. (14).

3.2 Non-Dimensionalization

The basic reference quantities used for non-dimensionalization of the basic quantities are; the equilibrium bond length between beads σ_o for the length, the temperature T, the viscosity of the arbitrary fluid μ_{ref} for the viscosity, the solvent density ρ_0 for the density, and the electron charge e for the bead charge. The other reference quantities are; $\epsilon_{ref} = k_BT$ for the energy ϵ, $\tau_{ref} = \mu_{ref}\sigma_o^3/k_BT$ for the time, $F_{ref} = k_BT/\sigma_o$ for the force, $\varphi_{ref} = k_BT/e$ for the electric potential, $\Gamma_{ref} = \mu_{ref}\sigma_0$ for the friction coefficient, and $\nu_{ref} = \mu_{ref}/\rho_0$ for the kinematic viscosity. The reference viscosity μ_{ref} must be chosen carefully, because it is

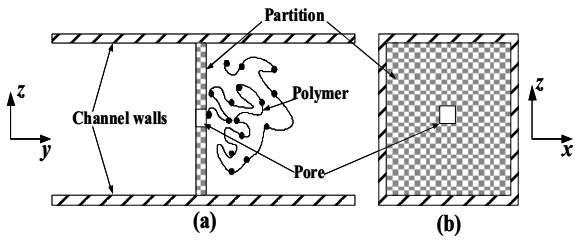

Fig. 3 Cross-sectional view of the simulation set-up at the center of (a) yz-plane and (b) xz-plane

related to the stability of the numerical scheme as well as the computational time. Suitable choice of this quantity is usually based on preliminary calculation of the developed code.

The relaxation time in LBM, which depends on the viscosity of fluid, is obtained from the non-dimensional variables by using the following formula.

$$\mu^* = \frac{\rho^* \triangle x^{*2}}{6 \triangle t^*}(2\tau - 1). \tag{15}$$

The lattice constant $\triangle x^*$is set to be unity. For stable and accurate lattice Boltzmann solution, the relaxation time τ should be close to 1. We first choose a suitable LB time step $\triangle t^*$, and then calculate the dynamic viscosity μ^* using (15).

The Langevin equations of motion, i.e., Eqs. (1a) and (1b), are solved numerically by using the stochastic position Verlet (SPV) algorithm [12] with a time step dt, which is a fraction of $\triangle t^*$. The time step ratio, $M = \triangle t^*/dt$ in our simulation is taken as 3. After several preliminary calculations we found that $dt^* = 0.01$ is suitable; the corresponding $\triangle t^*$ and μ^* are then 0.03 and 5 respectively.

3.3 POLYMER TRANSLOCATION

Figure 3 illustrates the cross-sectional view of the numerical set-up that is employed in this work. The simulations are performed inside a 3D square channel between two planar walls. A partition having a small square pore at the center is located at the midsection dividing the channel into two chambers. The wall/pore molecules are arranged in a simple cubic structure with spacing σ^*, which is equal to 1. The width of the pore is set as $3\sigma^*$, and length is $7\sigma^*$. The boundary conditions for the polymer motions are periodic in the y-direction, and the interactions with the wall molecules are given by

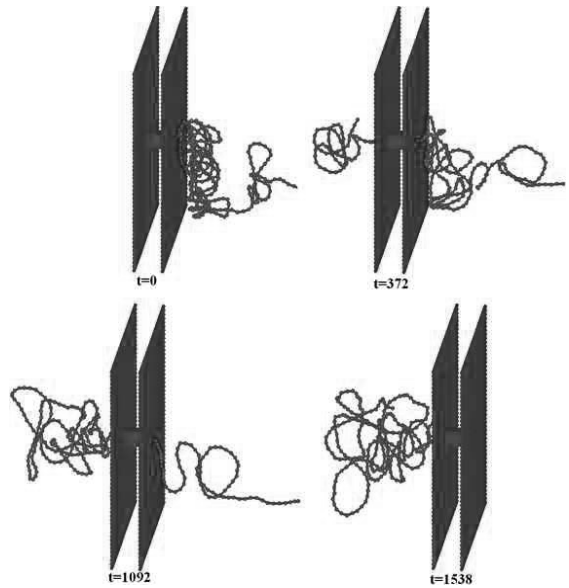

Fig. 4 Polymer configuration (N=300) of a translocation event at different times.

Lennard-Jones potential . For the fluid motion, the periodic boundary conditions are also given in the y-direction, and the standard mid-plane bounce-back scheme is employed at both the channel and partition walls.

The simulation parameters are chosen as follows. We set σ_o equal to 7.5 nm, so as the lattice grid size. The effective pore size in our simulations is approximately 10 nm as the interactions between the polymer beads and pore molecules are repulsive in nature. The pore size is comparable to that used in the experiments [13]. Since the bond length is 7.5nm, each bead in our simulations corresponds to 22 base pairs as the average distance between adjacent base pair in dsDNA is 0.34 nm. The friction coefficient for each bead is set from the diffusion coefficient D, using the relation,

$$\Gamma = \frac{k_B T}{D}. \tag{16}$$

The diffusion coefficient is obtained from $D = 7.73 \times 10^{-06} \times (N_b)^{-0.672}\ \mathrm{cm}^2/\mathrm{s}$ [14], where N_b is the number of base pairs. From Eq. (16), the calculated friction coefficient Γ^* of each bead in our simulation is around 20. Since DNA is kind of strongly charged polyelectrolyte, the effective charge reduces when it immersed in salt solution due to the counter ion condensation. According to Manning and Oosawa [15,16]

the charge of DNA, immersed in monovalent salt, is neutralized by 80%. So the effective charge along the DNA backbone is calculated from

$$q = 2(1-0.8)N_b|e| \tag{17}$$

where the factor 2 is included because of each base pair has two negatively charged phosphate groups. We assume that the effective charge is distributed uniformly along the backbone. The charge of the each bead in simulation is set to be $q^* = 8$. In experiments the voltage bias of 200 mV is applied across the pore. The corresponding potential difference in our simulation is set to be $\varphi^* = 8$. At the beginning of the translocation process the polymer resides on the right-hand side chamber of the channel as shown in Fig. 3. The applied electric field causes the polymer to translocate from right side to left side through nano-pore. Figure 4 shows the 3D configuration of a polymer with 300 beads at different time steps, while it is translocating through the pore.

4. CONCLUSIONS

In this work, we numerically investigated the electrophoretic motion of dsDNA through a nano-pore in three-dimensional space using a hybrid approach (LB and MD), which explicitly accounts HI of the polymer molecules with the surrounding fluid. The bead positions of the polymer are updated by numerically solving the Langevin equations of motion, while the fluid flow is taken into account by fluctuating LBE. The potential difference across the channel drives the DNA from one side of the channel to the other side through a nano-pore. In future we want to study the effect of the DNA chain length, and the electric potential difference on electrophoretic mobility.

ACKNOWLEDGEMENT

이 논문은 2009년도 교육과학기술부의 재원으로 한국연구재단의 지원을 받은'다중현상 CFD연구센터(ERC)'의 과제로 수행된 연구임(No.2009-0083510).

REFERENCES

[1] 1981, Lamm, G., and Shulten, K., "Extended Brownian Dynamics Approach to Diffusion Controlled Processes," *J. Chem. Phys*., Vol.75-1, p.365.

[2] 1992, Hoogerbrugge, P.J., and Koelman, J.M. V. A., "Simulating Microscopic Hydrodynamic Phenomena with Dissipative Particle Dynamics," *Europhys. Lett*., Vol.19, p.155.

[3] 1999, Malevanets, A. and Kapral, R., "Mesoscopic model for solvent dynamics," *J. Chem. Phys*., Vol.110-17, p.8605.

[4] 1999, Ahlrichs, P. and Dunweg, B., "Simulation of a single polymer chain in solution by combining lattice Boltzmann and molecular dynamics," *J. Chem. Phys*., Vol.111-17, p.8225.

[5] 2005, Usta, O.B., Ladd, A.J.C. and Butler, J.E., "Lattice-Boltzmann simulations of the dynamics of polymer solutions in periodic and confined geometries," *J. Chem. Phys*., Vol.122, p.094902.

[6] 1966, Kubo, R., "The fluctuation-dissipation theorem," *Rep. Prog. Phys*., Vol.29, p.255.

[7] 1971, Weeks, J D., Chandler, D. and Andersen, H. C., "Role of repulsive forces in determining the equilibrium structure of simple liquids," *J. Appl. Phys.*, Vol.54, p.5237.

[8] 1992, Benzi, R., Succi, S. and Vergassola, M., "The lattice Boltzmann-equation－Theory and applications," *Phys. Rep*., Vol.222, p.145.

[9] 2007, Premnath, K.N. and Abraham, J., "Three - dimensional multi-relaxation time (MRT) lattice-Boltzmann models for multiphase flow," *J. Comp. Phys*., Vol.224, p.539.

[10] 2002, Guo, Z., Zheng, C. and Shi, B., "Discrete lattice effects on the forcing term in the lattice Boltzmann method," *Phys. Rev. E*, Vol.65, p.046308.

[11] 1988, Flory, P.J., "Statistical Mechanics of Chain Molecules," *Oxford University Press*, New York.

[12] 2007, Melchionna, S., "Design of quasi-symplectic propagators for Langevin dynamics," *J. Chem. Phys*., Vol.127, p.044108.

[13] 2004, Chen, P., Gu, J., Brandin, E., Kim, Y., Wang, Q. and Branton, D., "Probing Single DNA Molecule Transport Using Fabricated Nanopores," *Nano lett.*, Vol.4-11, p.2293.

[14] 2003, Stellwagen, E., Lu, Y., Stellwagen, N.C., "Unified Description of Electrophoresis and Diffusion for DNA and Other Polyions," *Biochemistr,* Vol.42, p.11745.

[15] 1969, Manning, G.S., "Limiting laws and counterion condensation in polyelectrolyte Solutions. I. Colligative Properties," *J. Chem. Phys*., Vol.51, p.924.

[16] 1971, Oosawa, F., *Polyelectrolytes,* Marcel Dekker, New York.